(BL2A)

C_6F_5X (X = H, F, Cl, Br, and I) Excited Radical Cation Formation Efficiency in the 10-40 eV Region

T. Hikida[1], T. Ibuki[2], and K. Okada[3]

[1]*Department of Chemistry, Tokyo Institute of Technology, 152-8551*

[2]*Kyoto University of Education, 612-0863*

[3]*Department of Chemistry, Hiroshima University, 739-8526*

The fluorescence from $C_6F_5X^{+\cdot}$ (X=H, F, Cl, Br, and I) cation radicals were observed in the VUV photolysis of C_6F_5X (X=H, F, Cl, Br, and I) . The energy dependence of the excited radical formation were studied by the fluorescence excitation spectra (>400 nm) between 10 eV and 40 eV. Together with the absorption spectra, the fluorescence intensity efficiencies of the excited radical cations were determined as a function of excitation energy. The results are shown in the figure for $C_6F_5X^{+\cdot}$ (X=H, F, Cl, Br, and I).

The absolute emission cross-section was determined to be 17.5 $\pm$ 0.7 Mb for C_6F_5Cl at 21.22 eV. Then, the efficiency was calculated to be 0.10, knowing that the absorption cross-section of C_6F_5Cl at 21.2 eV is 170 Mb. Using this value and relative emission intensities, the absolute efficiencies of $C_6F_5X^{+\cdot}$ (X=H, F, Cl, Br, and I) were obtained. The vertical scales of the figure were thus determined.

All the samples showed clear thresholds at around 12 eV. The efficiencies increased and then remained nearly constant between 13 eV and 16 eV. The dark σ^{-1} excited state is energetically possible at 13.7, 13.9 and 12.4 eV for H, F, and Cl derivatives, but no such formation is indicated. Between 18 eV and 24 eV, another lower plateau appeared, and then gradually decreased to near zero for further increase in the excitation energy. The profiles of efficiency curves were very close for all the samples studied. Only the intensities varied. In table 2 are the summery of the thresholds and the fluorescence efficiencies of five samples.

The emission efficiency is given by the product of the formation efficiency and the emission quantum yield. Knowing the emission quantum yields (1.0), the formation of the excited radicals seem to be fairly effective. For X=H and F, 1.8% and 8% of absorbed photons in 13-16 eV should be converted to the excited radicals, respectively, and it may be very high, 18% or more for X=Cl. Very small efficiencies for $C_6F_5Br^{+\cdot}$ and $C_6F_5I^{+\cdot}$, however, are probably the reflection of small emission quantum yields. The dark σ^{-1} levels are lying below the emissive π^{-1} levels for these molecules. The absence of emission was often explained by the presence of energetically accessible σ^{-1} states near the emissive π^{-1} state.

The fluorescence quantum yields of $C_6F_5H^{+\cdot}$ and $C_6F_6^{+\cdot}$ measured by the photoelectron-photon coincidence experiments are reported to be strongly dependent on the excitation energy. For example, the quantum yield of $C_6F_6^{+\cdot}$ emission decreased from 1.0 at 12.5 eV to 0.25 at 13.3 eV. Further increase in the excitation energy, it decreased drastically to 0.01 at 13.9 eV and to near zero at 14.2 eV. The fluorescence excitation measurements did not show such phenomena.

The photoexcitation reactions should form the excited cation radicals with various vibrational energies. The

vibrational distribution of the photoproducts may be nearly constant for the 13-16 eV, and also for 18-24 eV regions. Excess energy should be removed by electron. It is interesting to note that the first portions of the efficiency curve where the efficiency is high and nearly constant is largely comprised of benzenic π orbital excitation. The second part of the curve is the same energy region as the absorption by the halogen lone pair. The last part where the efficiency is very low is probably the energy region of the inner shell excitation.

Table 1 Ionization energy and intensity threshold, and fluorescence efficiency.

	$C_6F_5X^{+\cdot}$	ionization energy (eV)		efficiency(%)	
		reported	this work	13-16 eV	18-24 eV
C_6F_5H	$\tilde{B}\ ^2B_1\ (\pi^{-1})$	12.50	12.49	1.8	0.85
C_6F_6	$\tilde{B}\ ^2A_{2u}(\pi^{-1})$	12.58	12.51	8.4	3.2
C_6F_5Cl	$\tilde{B}\ ^2B_1\ (\pi^{-1})$	12.20	12.17	18	10
C_6F_5Br	$\tilde{C}\ ^2B_1\ (\pi^{-1})$	11.90	12.12	0.13	0.08
C_6F_5I	$\tilde{C}\ ^2B_1\ (\pi^{-1})$	11.25	11.13	0.03	0.02

Fig.1 Fluorescence efficiency of $C_6F_5X^+$

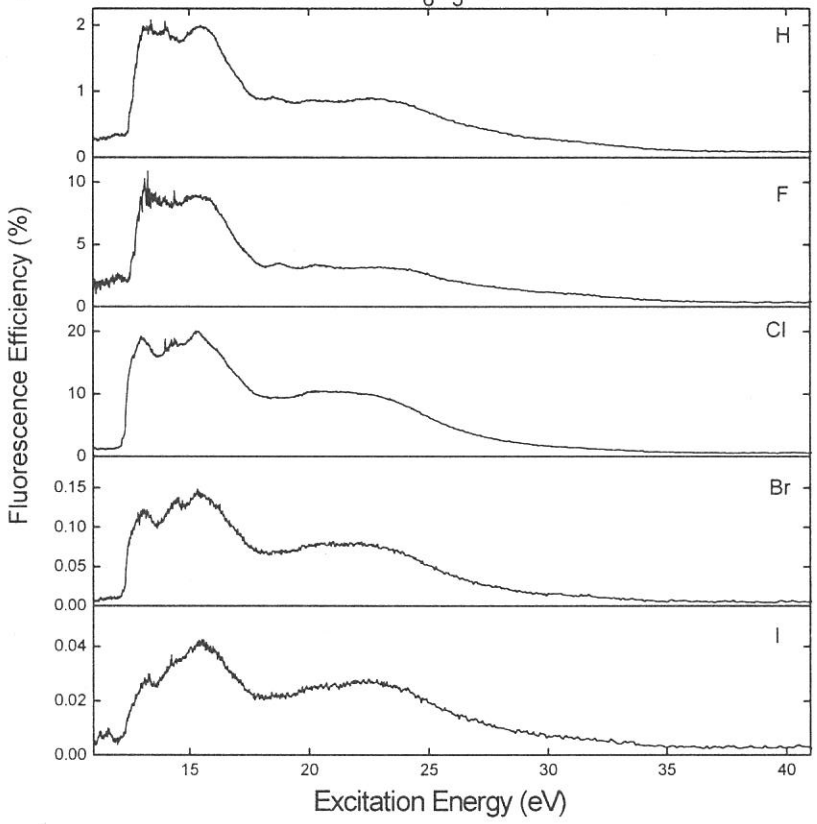

(BL2A)

Photoabsorption and Fluorescence Excitation Cross Sections of Butyl Cyanide and Butyl Isocyanide the VUV Region

Kazuhiro KANDA, Takashi NAGATA[A], and Toshio IBUKI[B]

Department of Fundamental Science, College of Science and Engineering, Iwaki Meisei University, Iwaki 970-8551

[A] *Institute for Molecular Science, Myodaiji, Okazaki 444-8585*

[B] *Kyoto University of Education, Fukakusa. Fushimi-ku Kyoto 612-0863*

A considerable amount of studies have been accumulated on the production of the excited CN radicals from cyanides by the VUV photoexcitation, however there have been scare reports on the photodissociative excitation of isocyanides. In the dissociative excitation by rare gas metastable atoms, the internal energy distributions of the produced CN($B^2\Sigma^+$) were reported to be much different in the case of isocyanides compared to the case of cyanides.[1] Deeper insight into the dissociation process requires the knowledge of the highly excited states in the VUV region. In the present study, photodissociation of relevant alkyl cyanides and isocyanides, *n*-C_4H_9CN, *t*-C_4H_9CN, *n*-C_4H_9NC and *t*-C_4H_9NC was investigated by the measurement of the photoabsorption spectrum and the fluorescence excitation spectrum for the CN($B^2\Sigma^+$-$X^2\Sigma^+$) emission in the wavelength range 105-165 nm. The photoabsorption cross section was obtained from the ratio of the vacuum UV photon fluxes measured with the sample gas on and off. The CN($B^2\Sigma^+$-$X^2\Sigma^+$) emission in the UV and visible region was monitored with a combination of a band-pass filter (Toshiba C-39A) and a photomultiplier (Hamamatsu R585). The absolute emission cross section, σ_{em}, was determined by a comparison of the intensity of the CN($B^2\Sigma^+$-$X^2\Sigma^+$) emission produced in the photodissociation of CH_3CN in the 105-150 nm region.[2]

Fig. 1 shows absorption (thin line) and fluorescence excitation (thick line) spectra of *n*-C_4H_9CN, *t*-C_4H_9CN, *n*-C_4H_9NC and *t*-C_4H_9NC. The absorption spectra of *n*-C_4H_9CN and *t*-C_4H_9CN showed only structureless broad bands. The broadening of the absorption band is consistent with our previous study on the photodissociative excitation of small nitriles.[3] On the other hand, numerous sharp peaks were observed in the absorption spectra of *n*-C_4H_9NC and *t*-C_4H_9NC. These peaks are assignable to the Rydberg transitions converging to the first and second ionization potentials. The absorption cross section increases toward shorter wavelength in the 105-165 nm region. In the fluorescence excitation spectra from *n*-C_4H_9CN and *t*-C_4H_9CN, no sharp peak was observed as well as the photoabsorption spectra. The structure in the CN($B^2\Sigma^+$) excitation spectra from *n*-C_4H_9NC and *t*-C_4H_9NC corresponds to the structure in the absorption spectra of these isocyanides. The absolute value of cross section for the CN($B^2\Sigma^+$-$X^2\Sigma^+$) emission is *n*-C_4H_9CN < *t*-C_4H_9CN << *n*-C_4H_9NC < *t*-C_4H_9NC, that is, σ_{em} from isocyanide is larger than that from relevant cyanide and σ_{em} from photodissociation of containing tertiary butyl group is larger than that from containing normal butyl group. Even maximum of Quantum yield for the production of CN($B^2\Sigma^+$) takes maximum, ≈0.1, at 142 nm of *t*-C_4H_9NC. Dissipation of available excess energy to the alkyl group restrains the production of excited CN radical, because the disposed

energy to the R-CN or R-NC bonding decreases. Normal butyl group is more effective heat bath than tertiary butyl group, because of its flexible structure. Relatively large quantum yield from isocyanide and sharp peaks in the absorption and fluorescence excitation indicate that a little excess energy was disposed to alkyl group. These differences between the case in the cyanide and isocyanide is considered to be ascribable to the lifetime in the excited dissociative state. Namely, dissociative time of the excited isocyanide is regarded to be so short that the available energy cannot disposed to the alkyl group sufficiently.

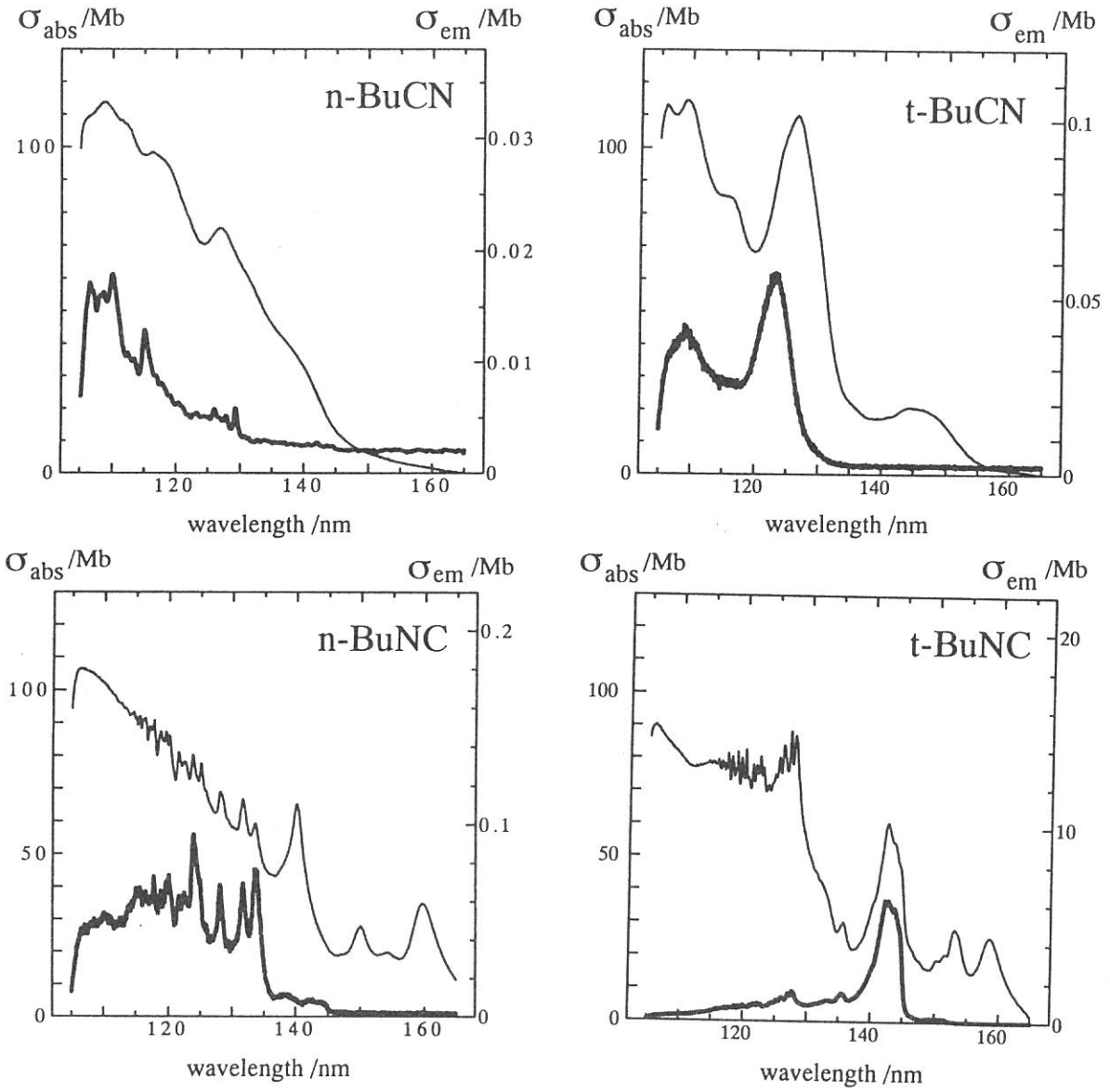

Fig. 1 The absorption and photoexcitation cross sections of n-C_4H_9CN, t-C_4H_9CN, n-C_4H_9NC and t-C_4H_9NC in the 105-165 nm region. The spectral resolution was 0.1 nm.

Reference

[1] K. Suzuki and T. Kondow, Atomic Collision Research in Japan, Progress Report, 16, 56 (1990).

[2] M. Kono, D. Thesis, Grad. Univ. Adv. Stud., (1995).

[3] K. Kanda et al., UVSOR Activity Report 1996, 82.

BL2A

Photoabsorption and Fluorescence Excitation of Formamide in the Vacuum Ultraviolet Region.

T. SUGIHARA, K. TABAYASHI, O. TAKAHASHI, K. SAITO, and T. IBUKI*

Department of Chemistry, Faculty of Science, Hiroshima University, Kagamiyama, Higashi-Hiroshima 739-8526

**Institute for Molecular Science, Myodaiji, Okazaki 444-8585*

Photochemistry of simple acid amides is of fundamental importance in connection with the photochemical properties of biological polymers, since they have the basic chromophoric unit in polypeptides. So far, photoabsorption spectra of the monomeric amides in the UV and VUV region have been accumulated, very little is known about the photochemical reaction initiated by UV and VUV photons. Here, fluorescence excitation cross section of formamide has been measured in the wavelength range 105-210 nm, dissociative excitation processes have been examined. The absorption bands are also reassigned based on the recent PES data and ab initio MO calculations.

The electronic configuration of $HCONH_2$ in the ground state is given by $(6a')^2(7a')^2(8a')^2(9a')^2(1a'')^2(10a')^2(2a'')^2$. The highest occupied 2a" and the next 10a' MOs have the π_{CO} and n_O characters, and are very close together in formamide. The absorption bands(solid line) and our assignments are shown in Fig. 1. The vibrational progressions in the Rydberg transitions have average spacings of ~530 and ~1600 cm^{-1}. They are assigned to NH_2 scissors and CO stretching vibrations from the vibrational analysis of the relevant ions by MO (HF/6-31G(d)) calculations.

Fig. 1 also shows the fluorescence excitation cross section(dotted line) obtained with detection of 370-850 nm radiation. The maximum cross section is found to be 0.044 Mb at λ_{exct} = 120 nm, which corresponds to the total quantum yield of 0.0023. The dispersed fluorescence measurement was not available due to low fluorescence intensity, excitation measurements were repeated with combinations of an optical filter and a PMT to cover different wavelength ranges in the 160–850 nm. From the comparison of these fluorescence excitation intensities, the dissociative excitation process,

$$HCONH_2 + h\nu \rightarrow HCO + NH_2(\tilde{A}\,^2A_1),$$

is concluded to be the most prominent fluorescent channel following the VUV excitation.

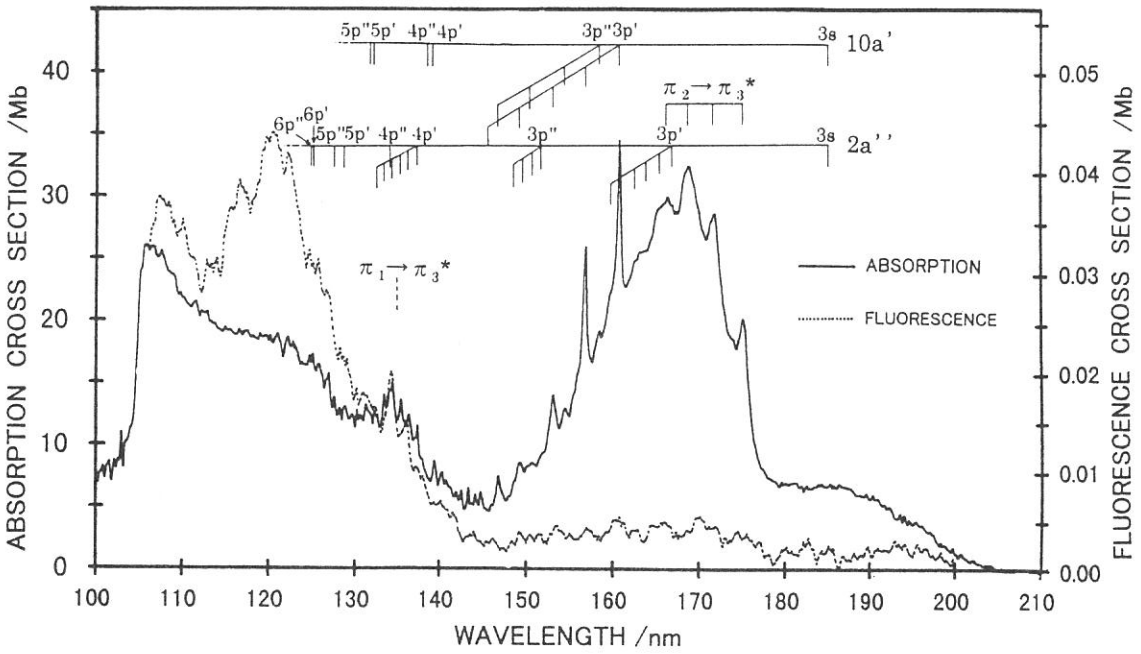

Fig. 1. Photoabsorption and fluorescence excitation cross sections for $HCONH_2$ in the 105-210 nm region. The spectral resolution was 0.2 nm. The sample pressure was 38 mTorr.

(BL3A2)

Anisotropic Angular Distribution of Ionic Fragments in the Dissociation of CO_2^{2+}

Toshio MASUOKA

Department of Applied Physics, Faculty of Engineering, Osaka City University, Sugimoto 3-3-138, Sumiyoshi-ku, Osaka 558-8585

Angular distributions of fragment ions ($O^+ + CO^+$ and $C^+ + O^+$) produced in dissociative double photoionization of carbon dioxide have been studied in the photon energy region 41-100 eV by use of a photoion-photoion coincidence (PIPICO) technique and a source of synchrotron radiation.

The spectral profiles of PIPICO peaks are determined by the kinetic-energy distribution and the angular distribution of the fragment ions, both with respect to the spectrometer axis, and other experimental conditions such as the electric field across the ionization region, the size and the degree of polarization of the photon beam and so on. In order to obtain the angular distribution of fragment ions, the kinetic-energy distribution was determined first by analyzing the PIPICO spectra measured at the so-called "pseudomagic angle," which is equal to about 55° under the assumed condition that the degree of polarization of the light $p = 0.9$ (Ref. 1).

The differential partial cross section of the fragment ions for the partially polarized light is given by

$$\frac{\partial\sigma_i}{\partial\Omega} = \frac{\sigma_i}{4\pi}\left[1 + \frac{\beta}{4}(3p\cos 2\theta + 1)\right]$$

in the frame work of the dipole approximation for randomly oriented molecules with cylindrical symmetry in the gas phase, where β is the asymmetry parameter that characterizes the angular distribution and θ is the angle of the spectrometer axis relative to the electric vector of the light.

The asymmetry β parameter was obtained by the following three steps. (1) Spectral profiles at $\theta = 0°$ and 90° were calculated for a set of various kinetic energies of the fragment ions with an arbitrarily fixed β parameter. (2) The spectral profile of the PIPICO peak at the angle θ was calculated, based on the kinetic-energy distribution already determined and the profiled calculated in step 1. (3) By treating the β value as a running parameter, its most probable value was determined as the one for which the sum of squares of the residuals between the observed and calculated profiles was minimized.

The observed β parameter is shown in Figs. 1 and 2 for $O^+ + CO^+$ and $C^+ + O^+$ channels, respectively, as a function of excitation energy. At low energy side close to the respective thresholds, the uncertainty in the β parameter is relatively large because of the poor counting statistics and the wavy background superposed on the PIPICO peaks. However, a clear trend in the β parameter can be seen as a function of excitation energy. For the $O^+ + CO^+$ channel, the mean value of the β parameter is close to 0.6 in the 47.5-60 eV region and is close to zero in the 70-100 eV region. For the $C^+ + O^+$ channel, the β parameter decreases as a function of excitation energy, which is the similar trend in the $O^+ + CO^+$ channel.

The observation of anisotropy in double photoionization from the valence orbitals of CO_2 will be discussed in relation to the symmetry consideration involved in the transition.

Reference

1) T. Masuoka, I. Koyano, and N. Saito, Phys. Rev. A 44, 4309 (1991).

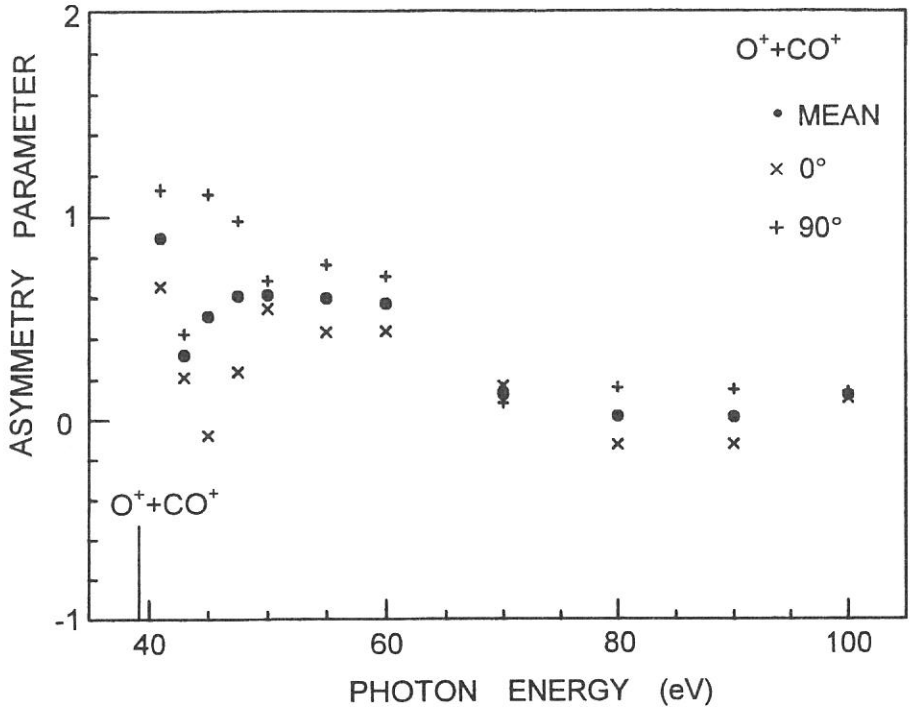

FIG. 1 Asymmetry parameter β for the $O^+ + CO^+$ dissociation channel of CO_2^{2+} measured at θ = 0° (×) and 90° (+).

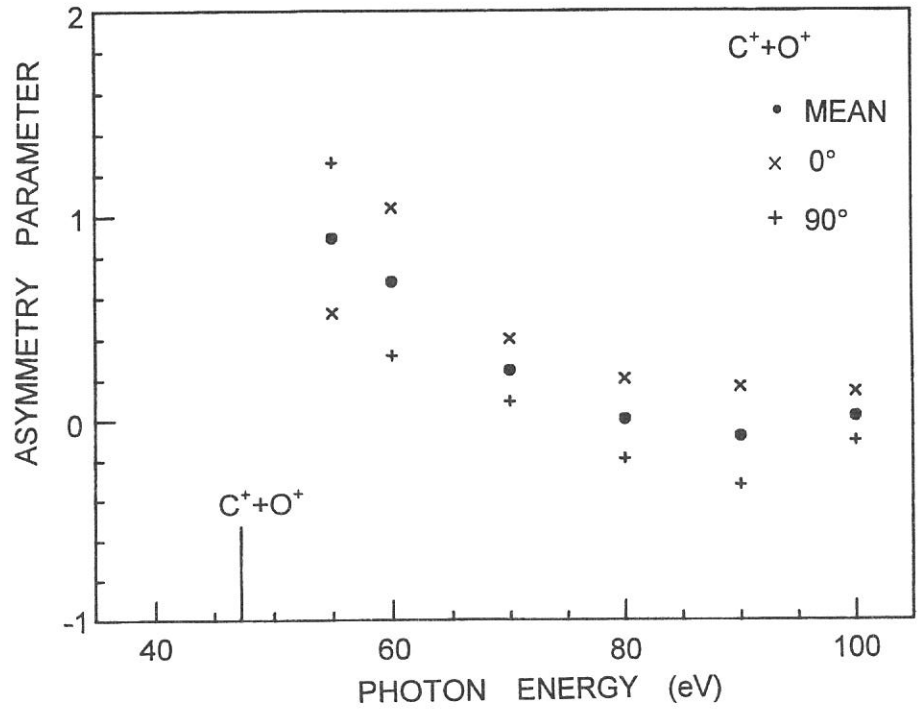

FIG. 2 Asymmetry parameter β for the $C^+ + O^+$ dissociation channel of CO_2^{2+} measured at θ = 0° (×) and 90° (+).

(BL3A2)

Dissociative Photoionization of Ferrocene in the Fe:3p Inner-Valence Region.

Yusuke Tamenori, and Inosuke Koyano
Departmentof MaterialScience, Himeji Institute of Technology, Kamigori, 678-12

In previous X-ray absorption and electron energy loss measurements on various transition metal compounds, it was suggested that the strong photoionization resonance can be found in the vicinity of metal np ionization threshold, which can be attributed to np transition to an unoccupied molecular orbital. However, there has been little information about ion fragmentation following the resonance transition. We are performing a series of detailed studies of dissociative photoionization of transition metal compounds in the inner valence region by use of TOF mass spectrometry and photoion-photoion coincidence technique (PIPICO).[1] In the present work, the dissociative photoionization of ferrocene ($Fe(cp)_2$) is studied in the range 37-100eV placing a special emphasis on the behavior in the vicinity of the Fe:3p ionization threshold (55eV).

Figure 1 shows an example of TOF mass spectrum taken at an incident photon energy of 50eV and a drift tube length of 20cm. The abundant ion is the parent ion ($Fe(cp)_2^+$) with some intensities for cp loss fragments($Fe(cp)^+$, Fe^+). The fragment ions originating from the ligand (C_nH_m n=2-5) are also observed with high abundances. However, owing to the closely spaced mass peaks, we can not distinguish between some different fragment ions. Such overlapped peaks are shown under a single label e.g. $C_3H_m^+$. Only one metastable doubly charged ion was observed at the mass number of 93, which is assigned to $Fe(cp)_2^{2+}$. Figure 2 present a PIPICO spectrum taken at 66eV of incident photons. The most abundant ion-pairs are those corresponding to the formula Fe^+-$C_3H_m^+$. Other ion-pairs involving $C_3H_m^+$ as a partner also give a high abundance. The relative intensity of ions and ion-pairs produced by the cp breakage is very high in contrast to the case of previous studies of metal-carbonyl compounds where simple ligand elimination is the dominant dissociation process.

Shown in Figure 3 are the incident photon energy dependences of the partial photoion yields of main observed ions. It is interesting to note that only the partial photoion yield of $Fe(cp)_2^{2+}/Fe(C_3H_3)^+$ shows the remarkable enhancement in the range from about 55eV to 70eV, which corresponds to the Fe:3p edge, whereas other ions are only slightly enhanced in this energy region. Although the observed variation is relatively small, the present result clearly indicates the occurrence of characteristic fragmentation following the resonance excitation. On the other hand, this result contrasts with the dissociative photoionization of metal-carbonyls in which the yields of almost all observed ions show an increase at the metal np edge. This difference may result from the difference in the mechanisms of intramolecular energy transfer through the metal-carbonyl and metal-cycropentene coordination bonds.

<Reference>

1, Y. Tamenori, K. Inaoka, and I. Koyano, *J. Electron Spectros. Rela. Phenom.* 79 , 503 (1996); Y. Tamenori, and I. Koyano, *J. Phys. Chem.* in press

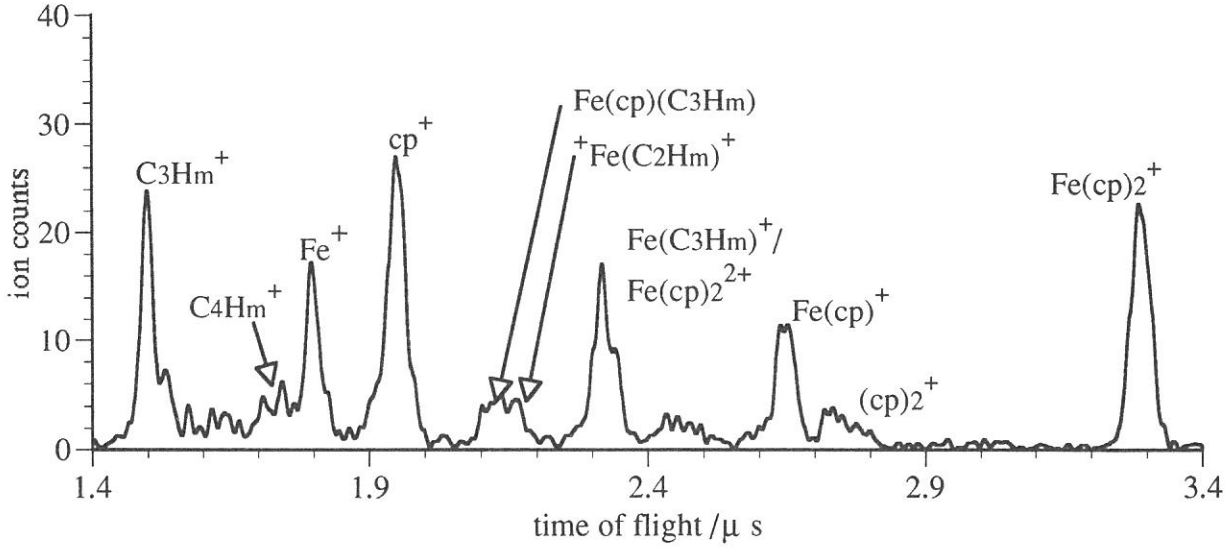

Figure 1, A TOF mass spectrum of ferrocene taken at 50eV of incident photon energy.

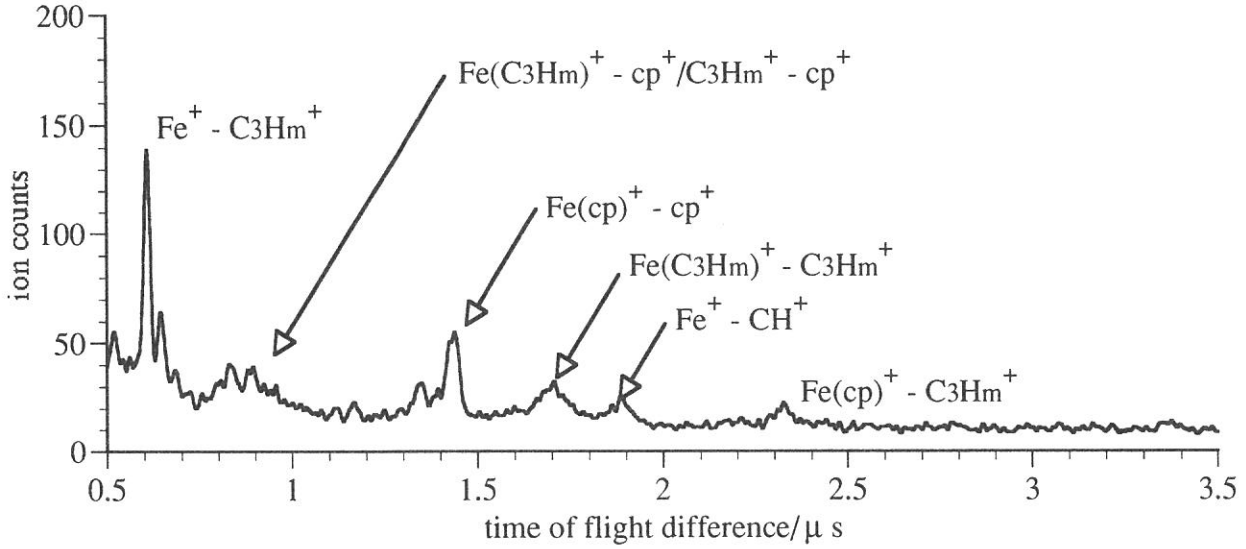

Figure 2, A PIPICO spectrum of ferrocene taken at 66eV of incident photon energy.

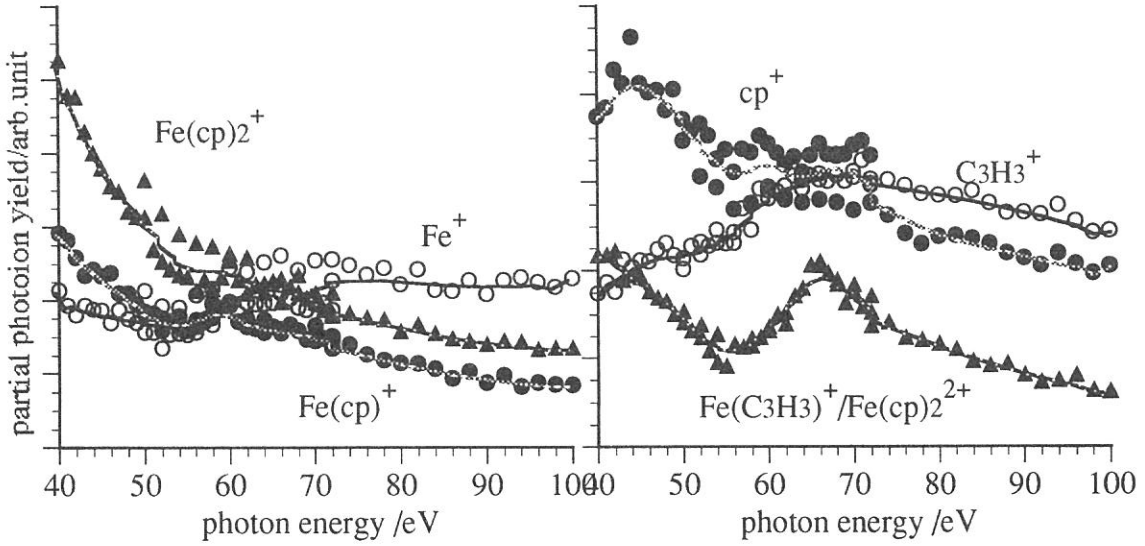

Figure 3, Incident photon energy dependence of the partial photoion yield of ferrocene.

(BL3A2)

Laser Induced Fluorescence Excitation Spectroscopy of N_2^+ Produced by Predissociation of N_2O^+ ($B\ ^2\Pi$).

Hiromichi Niikura*, Masakazu Mizutani**, Kota Iwasaki** and Koichiro Mitsuke**

*The Graduate University for Advanced Studies, **Institute for Molecular Science, Myodaiji, Okazaki, 444 - 8585, Japan.

Laser induced fluorescence (LIF) spectroscopy combined with synchrotron radiation (SR) photoexcitation has been exploited for investigating the internal energy distribution of fragment ions produced by VUV photoexcitation and the detailed mechanism for their formation.[1] In the present work, we measured the LIF yield curve of $N_2^+(X\ ^2\Sigma_g,\ v''=0)$ produced by the dissociative photoionization of N_2O with SR. The second harmonic of a Ti-sapphire laser was used to cause an excitation transition of $N_2^+(B\ ^2\Sigma_u,\ v'=0) \leftarrow N_2^+(X\ ^2\Sigma_g,\ v''=0)$. Then, fluorescence $N_2^+(B\ ^2\Sigma_u,\ v'=0) \rightarrow N_2^+(X\ ^2\Sigma_g,\ v''=1)$ at ~ 427 nm was monochromatized and detected.

Experimental details have been reported elsewhere.[1] The spectral band width $\Delta\lambda$ (FWHM) of SR was made to go up to 4 Å for getting a better signal-to-background ratio. In this resolution, the intensity was typically 3×10^{15} photons $cm^{-2}\ s^{-1}$. The average power of the second harmonic of the Ti-sapphire laser was 150 mW at 389 - 392 nm. Both the entrance and exit slit widths of the monochromator which monitors the fluorescence were reduced to 0.5 mm to eliminate the background emission from other species, dominantly from excited neutral fragments. The spectral resolution (FWHM) of the monochromator was 4 nm.

Figure 1 shows the yield curve of $N_2^+(X\ ^2\Sigma_g, v''=0)$ obtained by plotting the fluorescence intensities as a function of the SR photon energy in the range 18.4 - 19.8 eV. The wavelength of the laser was tuned at 391.5 nm which corresponds to the band head of the *P*-branch for the excitation $N_2^+(B\ ^2\Sigma_u,\ v'=0) \leftarrow N_2^+(X\ ^2\Sigma_g,\ v''=0)$. Several structures are identified to the $nd\pi$ Rydberg series converging to $N_2O^+(C\ ^2\Sigma^+)$ by comparing with the previous assignments,[2] while $nd\sigma$ Rydberg series are indiscernible. The mechanism for production of the fragment ion N_2^+ has been inferred[2] from its photoionization efficiency curve as follows:

$$N_2O + h\nu_{SR} \rightarrow N_2O^{**} \quad \text{(Excitation to a Rydberg State)} \quad (1)$$

$$N_2O^{**} \rightarrow N_2O^+(B\ ^2\Pi) + e^- \quad \text{(Autoionization)} \quad (2)$$

$$N_2O^+(B\ ^2\Pi) \rightarrow N_2^+(X\ ^2\Sigma_g) + O\ (^3P_g) \quad \text{(Predissociation)} \quad (3)$$

On the other hand, the contribution of direct ionization to N_2O^+ ($B\ ^2\Pi$) instead of processes (1) and (2) is considered to be small as actually expected from Fig. 1. The relative peak intensity appears to weakly depend on the principal quantum number of n = 3 - 6, and no marked difference in the intensity distribution is exhibited between the present LIF measurement and the previous mass spectrometric detection[2] of N_2^+.

In the future, this pump-probe technique combining SR excitation with LIF spectroscopy is expected to provide valuable information on vibrational and rotational energy distributions of fragment ions produced by photoexcitation and photoionization in the VUV region.

References

1) M. Mizutani, H. Niikura, A. Hiraya and K. Mitsuke, J. Synchrotron Rad., in press.

2) J. Berkowitz and J. H. D. Eland, J. Chem. Phys., **67** (1977) 2740

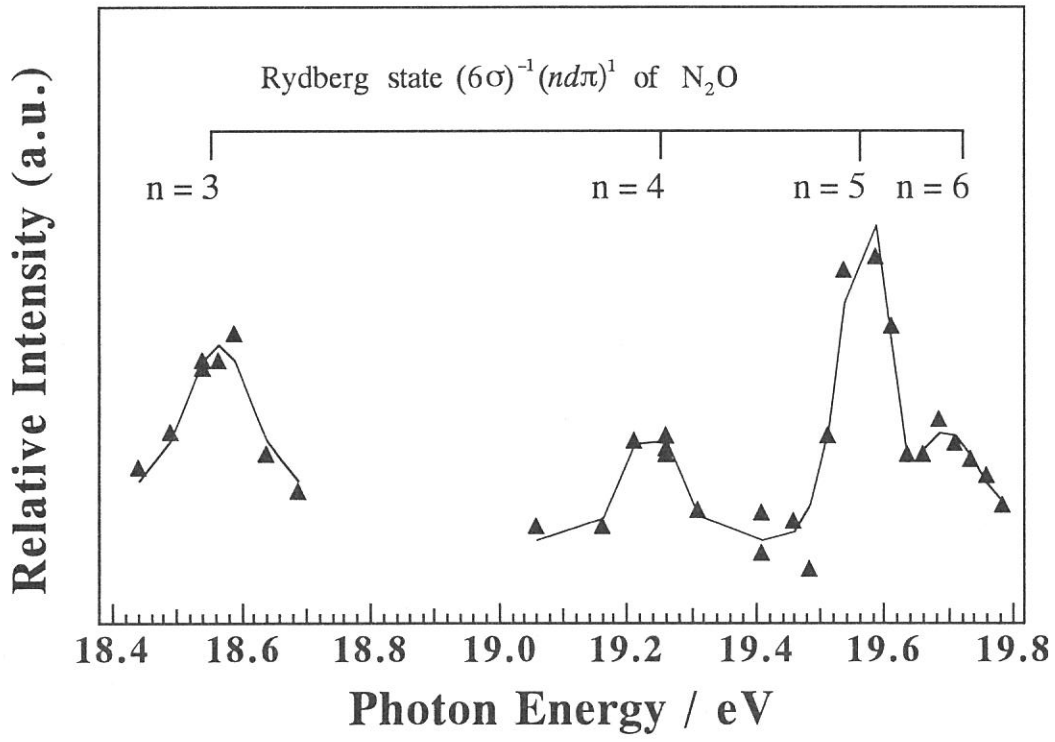

Figure 1. Photodissociation yield curve of $N_2^+(X\,^2\Sigma_g, v'' = 0)$ produced from N_2O obtained by plotting the LIF count rate as a function of the SR photon energy. The assignments of the $nd\pi$ Rydberg states converging to N_2O^+ $(C\,^2\Sigma_g^+)$ are indicated.

(BL3A2)

Laser Induced Fluorescence Excitation Spectroscopy of N_2^+ Produced by VUV Photoionization of N_2

Masakazu MIZUTANI, Hiromichi NIIKURA[A] and Koichiro MITSUKE

Department of Vacuum UV Photoscience, Institute for Molecular Science, Okazaki 444-8585, Japan
[A]The Graduate University for Advanced Studies, Okazaki 444-8585, Japan

In order to study the mechanism of dissociation of state-selected ions or neutral dissociation of superexcited molecules, a pump-probe experimental method combining synchrotron radiation excitation and laser-induced fluorescence (LIF) excitation spectroscopy has been developed. The main subject of this report is observation of the internal distribution of ions produced by VUV excitation by means of the LIF method.

As the most appropriate starting point, we have paid our attention to N_2^+ ions produced from N_2 by VUV photoionization with synchrotron radiation. The schematic diagram of the apparatus and detection system is shown in Figure 1. The fundamental light of the undulator radiation is monochromatized by a grazing-incidence monochromator (photon energy, E_{SR}) and introduced coaxially with the second harmonic of a mode-locked Ti:sapphire laser (Spectra Physics Lasers, Tsunami, 3950-L2S).[1] Sample gases, N_2, are photoionized preferentially into vibronically ground N_2^+ ions by irradiation of synchrotron radiation, and an LIF excitation spectrum of N_2^+ is measured in the laser wavelength region of the ($B\ ^2\Sigma_u^+$, $v' = 0$) ← ($X\ ^2\Sigma_g^+$, $v'' = 0$) transition at 389 - 392 nm. The fluorescence of the ($B\ ^2\Sigma_u^+$, $v' = 0$) → ($X\ ^2\Sigma_g^+$, $v'' = 1$) transition at about 427 nm is dispersed by another monochromator and detected with a photomultiplier (Hamamatsu, R464S).

Figure 2 shows an LIF excitation spectrum of N_2^+ produced by photoionization of N_2 at $E_{SR} = 15.98$ eV. Since this photon energy agrees with the resonance energy for the $4d\sigma_g$, $v = 0$ state converging to N_2^+ ($A\ ^2\Pi_u$), most of N_2^+ ions are produced by autoionization of this Rydberg state. The LIF excitation spectrum exhibits two maxima due to the *P* and *R* branches in which rotational bands are heavily overlapped. The rotational temperature is approximated by simulating the LIF excitation spectrum by using the theoretical intensity distribution of rotation bands convoluted with the present laser spectral width of 9.2 cm^{-1}. In Figure 2 a calculated spectrum at $T = 300$ K is indicated by a solid line. Experimental data points appear to gather around this curve. This suggests that rotational excitation in N_2^+ ($X\ ^2\Sigma_g^+$, $v'' = 0$) is not particularly induced through autoionization of the $4d\sigma_g$ Rydberg state. Similar results have been obtained on direct ionization of N_2 at $E_{SR} = 18$ eV.[2]

In the near future, we will study the decay dynamics of vibronically excited ions by means of single vibronic level dispersed fluorescence spectroscopy of an excited state produced by laser excitation of ground-state ions prepared by VUV photoionization.

References

1) M. Mizutani, M. Tokeshi, A. Hiraya and K. Mitsuke, J. Synchrotron Radiation **4**, 6 (1997).
2) M. Mizutani, H. Niikura, A. Hiraya and K. Mitsuke, J. Synchrotron Radiation **5**, (1998) *in press.*

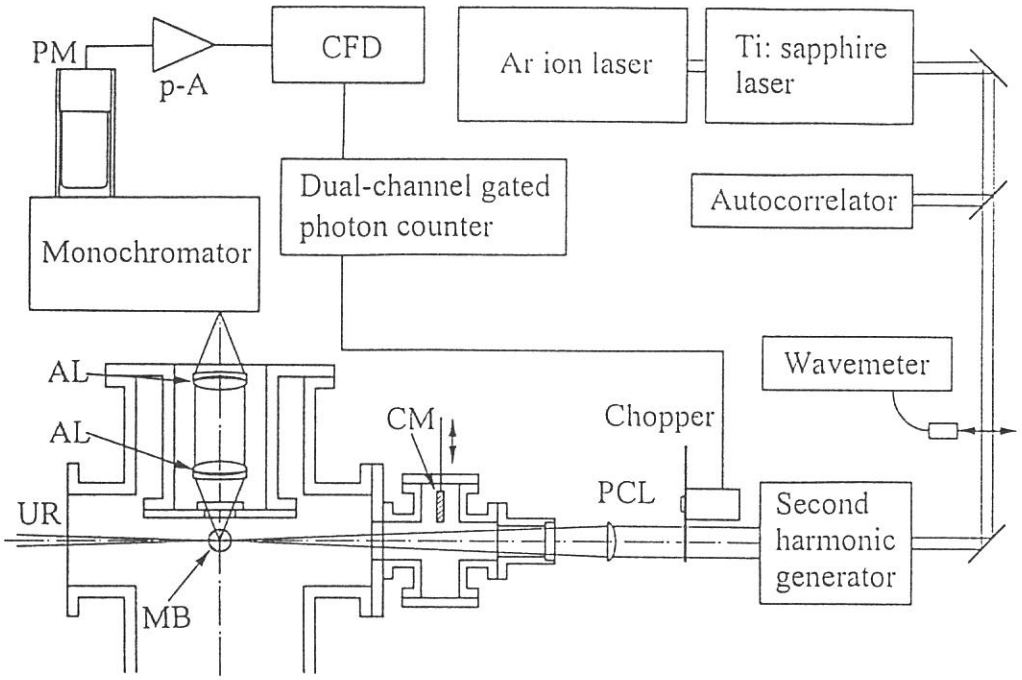

Figure 1. Schematic arrangement of the apparatus for synchrotron radiation-laser combination experiments. PM, photomultiplier; p-A, pre-amplifier; CFD, constant fraction discriminator; AL, spherical achromatic lenses; UR, monochromatized undulator radiation; MB, cross section of a molecular beam expanded from a nozzle; CM, gold-mesh current monitor; PCL, spherical plano-convex lens.

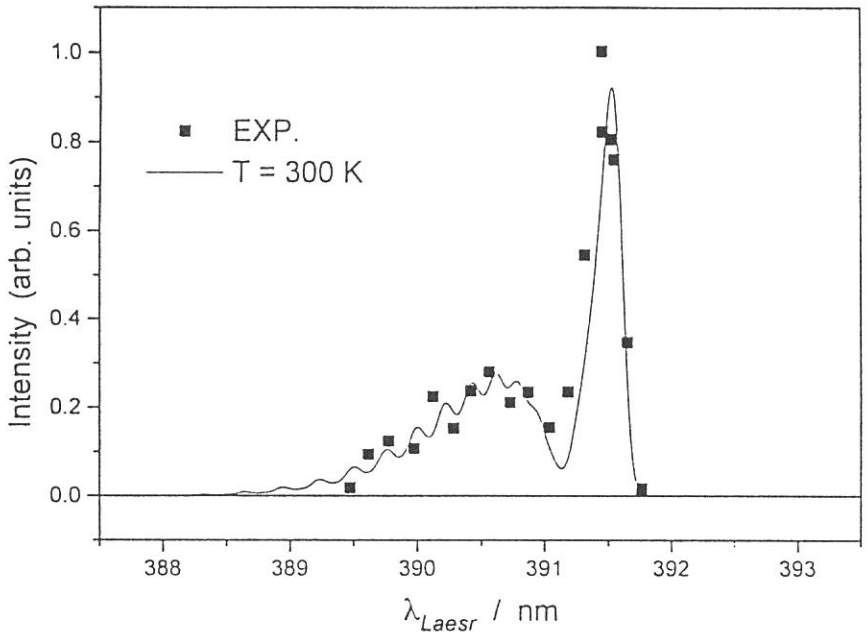

Figure 2. Laser induced fluorescence excitation spectrum of the $(B\,^2\Sigma_u^+,\ v' = 0) \leftarrow (X\,^2\Sigma_g^+,\ v_i'' = 0)$ transition of N_2^+ which is prepared by photoionization of N_2 at E_{SR} = 15.98 eV. The monitored fluorescence at 427 ± 4 nm is ascribed to the $(B\,^2\Sigma_u^+,\ v' = 0) \rightarrow (X\,^2\Sigma_g^+,\ v_f'' = 1)$ transition. The solid line represents a spectrum at T = 300 K calculated by using the theoretical intensity distribution of rotation bands convoluted with the laser spectral width of 9.2 cm^{-1}.

(BL3B)

Two-Photon Ionization Photoelectron Spectroscopy of Ar Using Visible laser and Synchrotron Radiation

Yasumasa HIKOSAKA and Koichiro MITSUKE

Department of Vacuum UV Photoscience, Institute for Molecular Science, Okazaki 444-8585 Japan

There has been a growing interest in deactivation mechanism of molecular excited states lying in the vacuum ultraviolet region. Neutral dissociation is one of major decay processes from these states. The neutral dissociation frequently yields a pair of fragments which are free from both autoionization and radiative decay and therefore difficult to detect. In order to obtain an understanding of the dissociation dynamics, we have developed a laser-synchrotron radiation (SR) combination system to conduct two-photon ionization photoelectron spectroscopy, where fragments produced by neutral dissociation are probed by laser ionization.

The geometry of the experimental setup is schematically depicted in Fig. 1. Sample gas is admitted into an ionization cell through a 1-mm diameter pipe at room temperature. The SR is dispersed using a 3 m normal incidence monochrometor and is introduced into the cell. The light beam of a frequency-doubled Nd:YAG laser (532 nm) with the repetition of 8 KHz intersects perpendicularly with the SR beam in the ionization chamber. The electric vector of the laser beam is perpendicular to that of the SR beam. A 160 ° spherical electrostatic electron energy analyzer with the mean radius of the electron orbit of 54.7 mm is placed in the parallel direction to the electronic vector of the SR beam. Energy-analyzed electrons are detected by a position sensitive detector composed of dual microchannel plate multipliers and a two-dimensional resistive anode encoder. In order to improve the signal to background ratio, the detection of electrons is inhibited when the laser is off.

Laser photoelectron spectroscopy of Ar Rydberg states has been carried out to check the performance of the present system. The Rydberg states are prepared by irradiation of the SR beam. Photoelectron spectra are measured consecutively at SR wavelength intervals of 0.3 Å in a region where the $Ar^*(3p^5 3d)$ and $Ar^*(3p^5 5s)$ states lie, and the electron yield is plotted as a function of both photon energy of SR and kinetic energy of the electron. This method is what is called two-dimensional photoelectron spectroscopy (2D-PES), and very useful for elucidating the dynamics of superexcited states.[1] Figure 2 shows the measured 2D-PES. When the photon energy of SR is tuned at the $Ar^*(3p^5 3d)$ states, increase in electron counts due to laser ionization into $Ar^+(^2P_{1/2})$ or $Ar^+(^2P_{3/2})$ are observed at specific kinetic energies. The $Ar^*(3d[1/2]_1)$ state, which is a Rydberg state converging to $Ar^+(^2P_{3/2})$, obviously results in not only $Ar^+(^2P_{3/2})$ but $Ar^+(^2P_{1/2})$. This fact indicates that the Rydberg electron does not preserve the spin momentum and/or that the Rydberg electron does not alter the angular momentum by ±1 on photoionization. No photoelectron signals from $Ar^*(3p^5 5s)$ states are detected on the 2D-PES, since angular distribution of the 5s electron is isotopic and hence the electrons through laser ionization is emitted in the parallel direction to the electronic vector of the laser.

[1] for example, Y. Hikosaka, H. Hattori, T. Hikida, and K. Mitsuke, J. Chem. Phys. **107**, 2950 (1997).

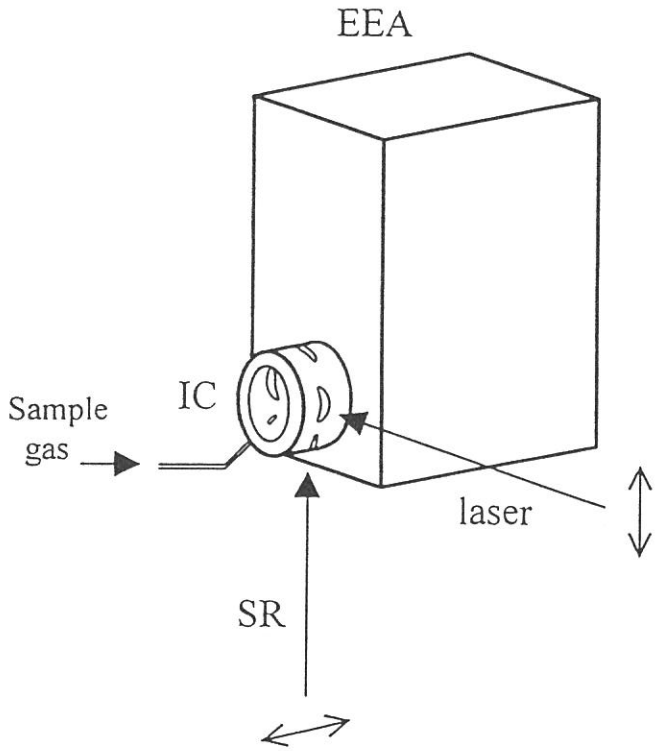

Figure 1 Geometry of the experimental setup. The synchrotron radiation (SR) beam is introduced into the ionization cell (IC) in the perpendicular direction to the laser beam. The electron energy analyzer (EEA) is placed in the parallel direction to the electronic vector of the SR beam.

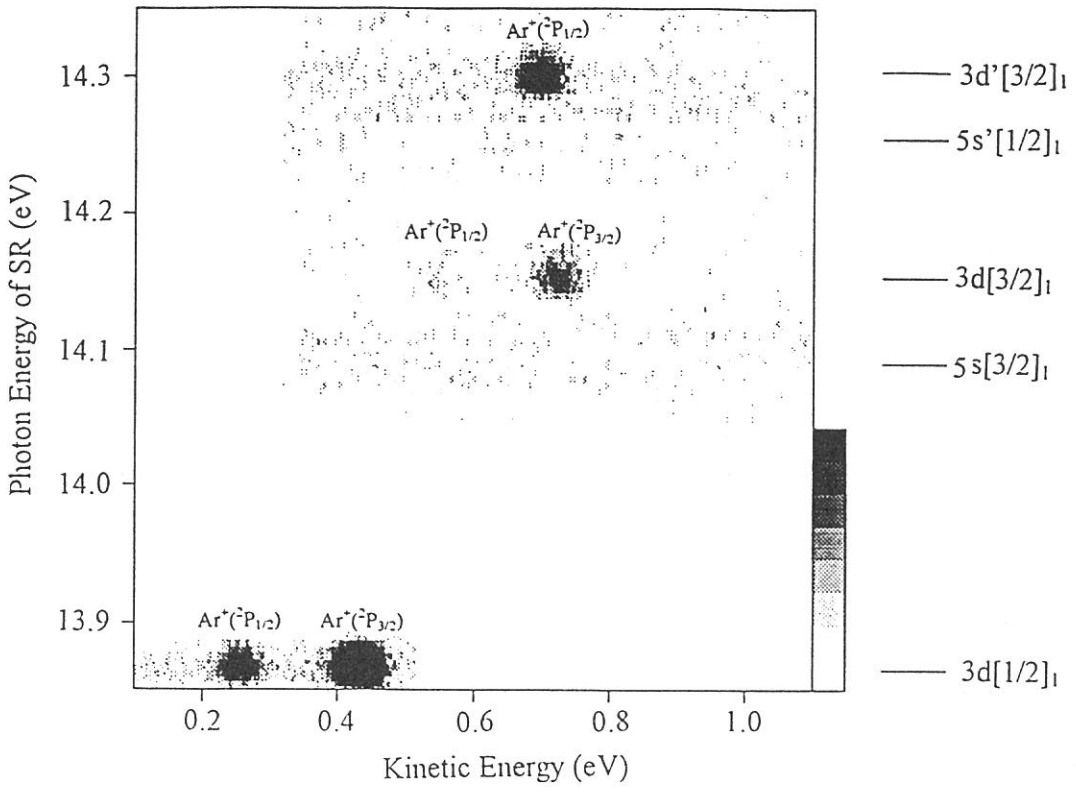

Figure 2 Two-dimensional photoelectron spectrum of Ar Rydberg states prepared by SR irradiation. The electron yield is presented by the plots with eight tones from light to dark on a liner scale.

(BL3B)

Autoionization of Superexcited Sulfur Atoms Produced from Doubly Excited Rydberg States of SO_2

Hideo HATTORI, Yasumasa HIKOSAKA, and Koichiro MITSUKE

Institute for Molecular Science, Myodaiji, Okazaki 444-8585, Japan

It is well known that superexcited states play important roles in molecular photoexcitation processes in the extreme ultraviolet (EUV) region. In particular, excitation of an inner valence electron or double-electron excitation are possible in the photon energy above 20 eV, and information on such processes is essential for a complete understanding of the molecular processes in the EUV region. However, our knowledge to date on superexcited states above 20 eV has been quite limited owing to their rapid decay and interference of a large cross section for direct photoionization. In this work, we have measured photoelectron spectra using synchrotron radiation in order to investigate doubly excited states and their decay of SO_2.

The experiment was carried out at the beamline BL3B in the UVSOR facility. Synchrotron radiation was dispersed by a 3-m normal incidence monochromator, and was focused onto a photoionization region. Photoelectron spectra of SO_2 were measured using a 160° concentric energy analyzer.

Figure 1 shows a photoelectron spectrum of SO_2 taken at the photon energy of 26.3 eV. Several sharp peaks are observed at the electron energy below 1.8 eV. These peaks have not been observed in He(II) photoelectron spectra previously reported, and cannot be assigned to any electronically excited states of SO_2^+.

Photoelectron spectra of SO_2 are measured at several photon energies between 22 and 32 eV. Three typical spectra are shown in Figure 2. It is found that some peaks appear at constant electron kinetic energies, which are independent of the photon energy. We have recently reported similar peaks in the photoelectron spectra of OCS, and attributed them to autoionization of superexcited sulfur atoms produced by neutral dissociation of superexcited states of OCS.[1] From comparison with the results of OCS, the peaks in Figure 2 are assigned to Rydberg states converging to $S^+(^2D^o)$, the first excited ionic state. Thus, the superexcited sulfur atoms are considered to be produced from SO_2 via the following processes:

1) $SO_2 + h\nu \rightarrow SO_2^{**}$ (Formation of a superexcited state)
2) $SO_2^{**} \rightarrow S^{**} + 2O$ (Neutral dissociation into three bodies)
   $\rightarrow S^{**} + O_2$ (Neutral dissociation into two bodies)
3) $S^{**} \rightarrow S^+ (^4S^o) + e^-$. (Autoionization of a superexcited sulfur atom)

Figure 3 shows a constant kinetic energy spectrum obtained by fixing the electron energy at 0.99 eV, corresponding to the formation of $S^{**}(4d\ ^1D^o)$. The spectrum indicates an onset at around 22.4 eV, where the lowest three-body dissociation limit $S^{**}(4d\ ^1D^o) + O(^3P^e) + O(^3P^e)$ lies. This suggests that S** atoms are mainly produced by the three-body dissociation, rather than by the two-body dissociation.

Furthermore, Figure 3 demonstrates a broad enhancement at 23 - 31 eV. Since previous photoelectron spectra have revealed the existence of satellite states of SO_2^+ in the ionization energy of 23 - 38 eV,[2] it is most likely that a number of doubly excited Rydberg states converging to the satellite states of SO_2^+ are responsible for the production of S**.

Reference

1) Y.Hikosaka, H.Hattori, T.Hikida, and K.Mitsuke, *J. Chem. Phys.* **107**, 2950 (1997).
2) D.M.P.Holland, M.A.MacDonald, M.A.Hayes, P.Baltzer, L.Karlsson, M.Lundqvist, B.Wannberg, and W.von Niessen, *Chem. Phys.* **188**, 317 (1994).

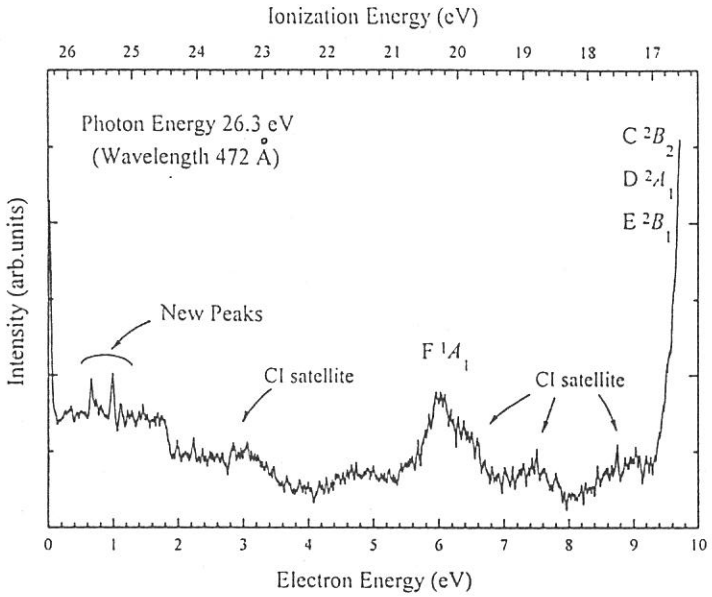

Figure 1. Photoelectron spectrum of SO_2 taken at the photon energy of 26.3 eV.

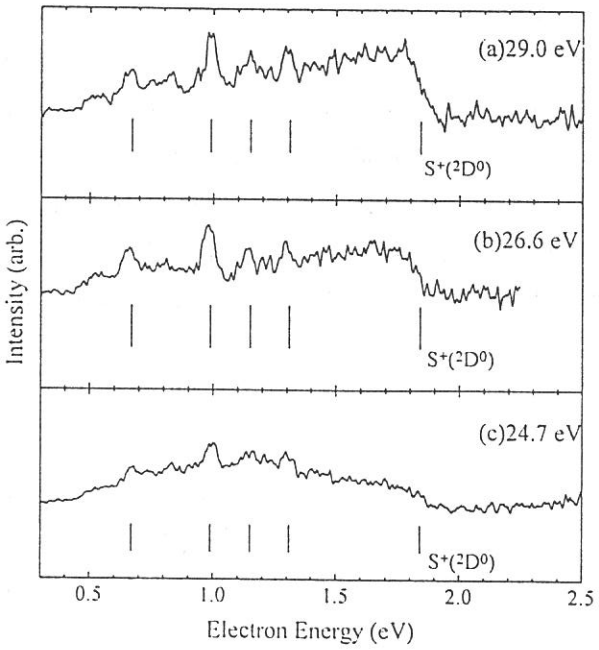

Figure 2. Photoelectron spectra of SO_2 at the photon energy of (a) 29.0, (b) 26.6, and (c) 24.7 eV. The vertical lines at 0.67, 0.99, 1.15, and 1.31 eV indicate the peaks appearing at constant electron energies, and are assigned to $5p^1F^e$, $4d^1D^o$, $6p^1F^o$, and $5d^1D^o$ states converging to $S^+(^2D^o)$, respectively. The vertical lines at 1.84 eV indicate the convergence limit of $S^+(^2D^o)$.

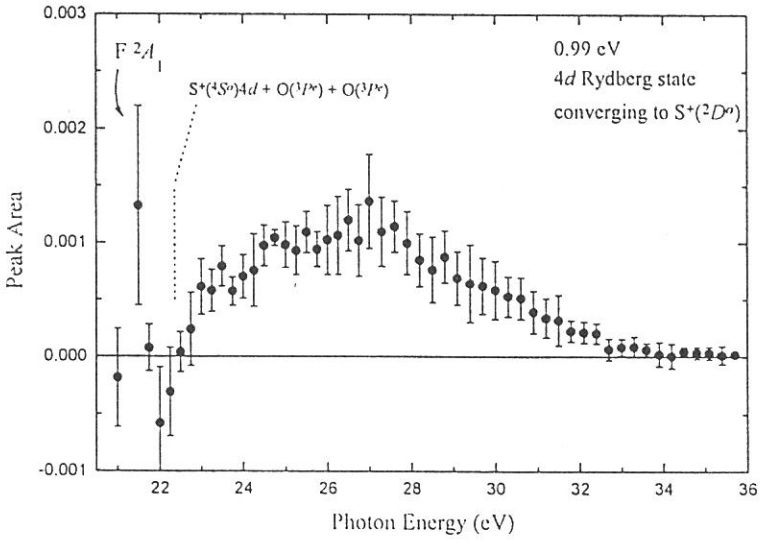

Figure 3. Constant kinetic energy spectrum for the peak at 0.99 eV in Figure 2 corresponding to the formation of the $4d\ ^1D^o$ state. The error bars represent standard deviations. The lowest limit for the three-body dissociation is indicated by the dotted line.

(BL8B1) **N AND C *K* SHELL EXCITATION OF CYANO BENZENES**

Toshio Ibuki, Kazumasa Okada[a], and Tatsuo Gejo[b]

Kyoto University of Education, Fukakusa, Fushimi-ku, Kyoto 612-0863
[a] Department of Chemistry, Hiroshima University, Higashi-Hiroshima 739-8526
[b] Institute for Molecular Science Myodaiji, Okazaki 444-8585

C_6H_5CN, C_6F_5CN, and p-$CF_3C_6H_4CN$ cyano benzenes have been excited at the N and C *K* shells on the soft X-ray beamline BL8B1. 3-Trifluoreomethylphenyl isocyanate, 3-$CF_3C_6H_4NCO$, was selectively exited at the N and O *K* shells. Reflectron type time-of-flight (R-TOF) mass spectrometer was installed to the main chamber to get a high resolution in mass separation. The main chamber is rotatable from –20 to 110° with respect to the electronic vector of the linearly polarized synchrotron radiation. The R-TOF mass spectra were measured at the magic angle in the present work.

The total photoabsorption (and also photoion yield) spectra of the cyano benzenes showed the distinct two or three peaks in the C and N *K* shell regions. The main band of C_6F_5CN in fig. 1, for example, would be assigned as the π*(C≡N)←N(1s) excitation. At the C *K* shell excitation the main band may be assigned as the transition to the vacant π* molecular orbital of the carbon atoms forming the phenyl group in molecule. The fragment patterns were compared between the π*←N(1s) around 400 eV and the π*←C(1s) at ≈285 eV excitations. Figure 2 shows the mass spectra measured at the π*←N(1s) resonance excitations. The difference between the two excitation modes, i.e., the π*←N(1s) and π*←C(1s), was quite small in the cyano benzenes. In the N *K* shell excitation of 3-$CF_3C_6H_4N$=C=O the small fragment ions such as H^+, N^+, O^+, N^+, and CF^+ were more produced than the terminal π*←O(1s) excitation at 530 eV, in which the relatively large fragment ions, CF_3^+, CF_2^+, and $C_6H_i^+$, survive.

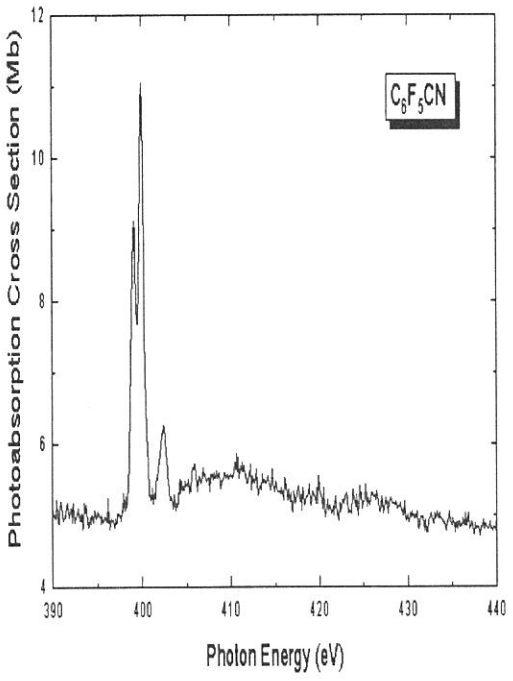

Fig. 1. Photoabsorption cross section of C_6F_5CN at the N *K* shell region.

The present observations suggest that the intramolecular energy redistribution in the *K* shell excited cyano benzene is extremely fast. In order to study the site-dependent photofragmentation it may be better to employ an aliphatic compound with functional group(s) since the selective excitation of –N=C=O group in 3-$CF_3C_6H_4NCO$ showed non-statistical

character, though it was weak.

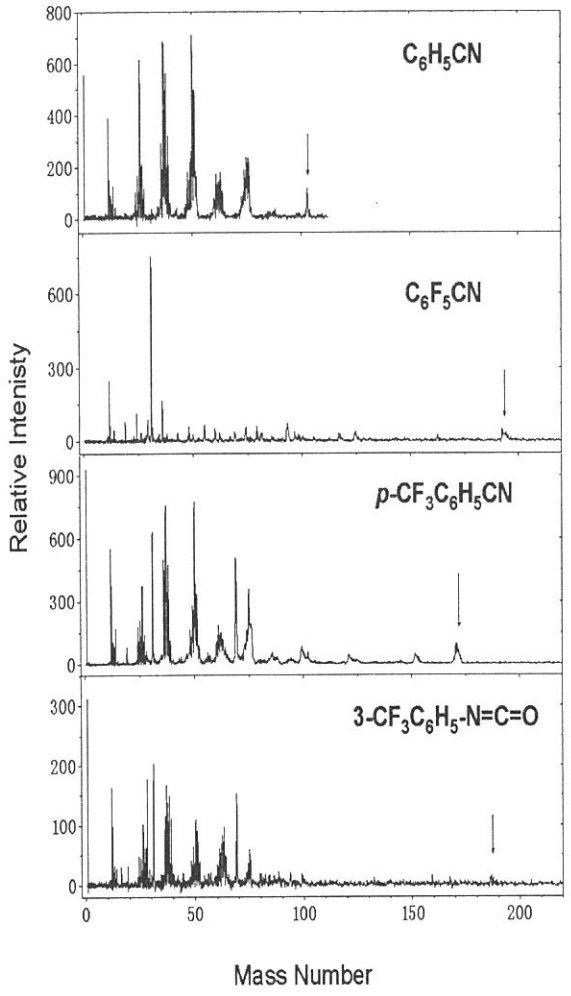

Fig. 2. R-TOF mass spectra excited at the $\pi^* \leftarrow$ N(1s) transitions. Arrows indicate the parent ions.

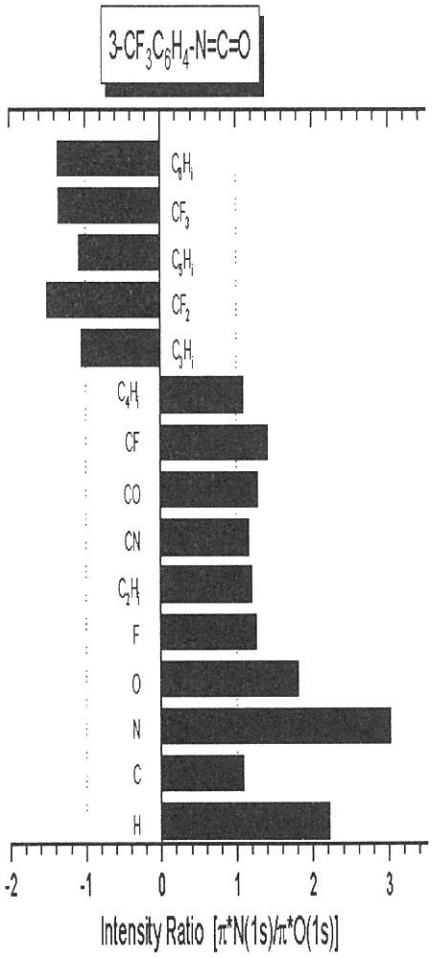

Fig. 3. Intensity ratios of the fragment ions formed at the N(1s) excitation to those at the O *K* shell excitation of 3-$CF_3C_6H_4NCO$. The fragment ions on the positive side indicate they are more produced at the central N(1s) excitation.

(BL8B1)

Photoabsorption Spectrum of Ozone in the K-edge Region

Tatsuo GEJO, Kazumasa OKADA[A] and Toshio IBUKI[B]

Institute for Molecular Science, Myodaiji, Okazaki 444-8585, Japan

[A]Department of Chemistry, Hiroshima Univ., Higashi-Hirosima 739, Japan

[B]Kyoto Univ. of Education, Fukakusa, Fushimi-ku, Kyoto 612, Japan

Ozone is one of the most important molecules in chemistry since ozone in the stratosphere absorbs UV light emitted from the sun and prohibits humanity from the exposure by the UV light. In view of this ozone effect, many experimental and theoretical exertions have been devoted to the spectroscopic studies of ozone. However, highly electronically excited states of ozone have not been fully understood yet nor have the spectroscopic data exceeding 20 eV been reported so far as we know. In order to explore the electronic states of ozone by the O(1*s*) core excitation, we have constructed an ozone supply apparatus on the beam line BL8B1. As a result, the photoabsorption and total electron yield spectra of ozone have been successfully measured for the first time in the soft-X-ray region 520-555 eV.

The photoabsorption spectrum have been measured at BL8B1. A photoabsorption cell was 25.0 cm long, which was attached to the main chamber. The typical sample pressure in the cell was 25 Pa measured by a Baratron manometer. An aluminum thin filter with a thickness of 100 nm was installed in front of the cell in order to keep the monochromator in high vacuum. The intensity of photon beam transmitted through the cell was monitored by using a silicon photodiode (IRD AXUV-100). The photoabsorption cross sections were calculated by using the Beer-Lambert expression. The data were checked to ensure that there is no line saturation effect.

The total photoabsorption cross sections of O_3 is shown in fig. 1. The corrected cross section was obtained after removal of the contribution from the coexisting O_2 component, assuming that the peak at 530.9 eV was a pure $\pi^*\leftarrow$O(1*s*) transition of O_2. The reported ionization potentials (IPs) of the O(1*s*) electrons in ozone are indicated by arrows. Fig. 1 is the first report for the absolute total photoabsorption cross section of O_3 in the soft X-ray region.

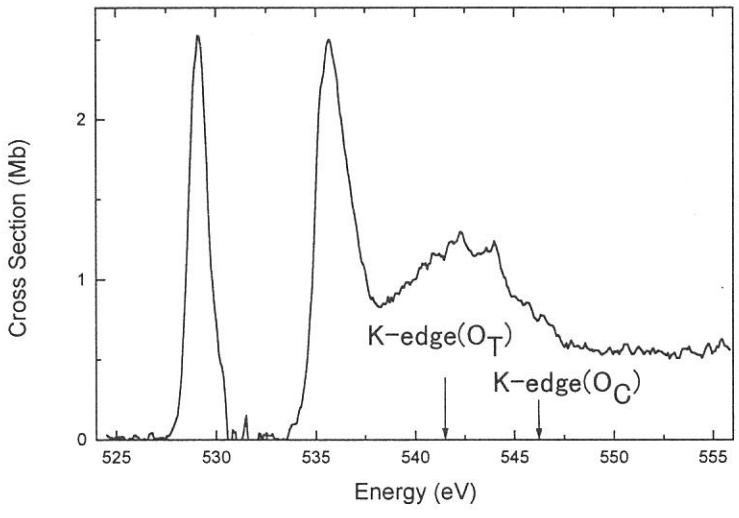

Fig. 1. Total photoabsorption cross section of ozone in the 525-555 eV energy region. Arrows show the ionization potentials of the 1s electrons at 541.5 and 546.2 eV obtained by XPS[1] of O_3.

The configuration of a molecular orbital (MO) representation in the ground state O_3 is:

Core: $1a_1^2 2a_1^2 1b_2^2$

Valence: $3a_1^2 2b_2^2 4a_1^2 5a_1^2 3b_2^2 1b_1^2 1a_2^2 4b_2^2 6a_1^2$

Vacant: $2b_1^0 7a_1^0 5b_2^0$

where the innermost $1a_1$ MO corresponds to the 1s orbital of the central oxygen atom, and the degenerate $2a_1$ and $1b_2$ MO's are almost even and odd combinations of the terminal O(1*s*) orbitals, respectively. Although the $2b_1(\pi^*)$ MO is vacant in the closed shell description, it has to be treated on an equal footing with the $1a_2$ MO because of the π biradical nature. The $7a_1$ MO is the lowest vacant σ^* level.

Two peaks definitely appear at 529 and 536 eV in fig. 1. Strong $\pi^* \leftarrow$O(1*s*) transition probability has been commonly observed at $\approx$ 530 eV in the O(1*s*) core-excitation of the compound containing O-atom. We assign the first distinct peak at 529.1 eV to be the $\pi^*(2b_1) \leftarrow 1s(2a_1)$ resonance excitation of the terminal oxygen atom of O_3 since the IP of the terminal O(1*s*) atom lies 4.7 eV lower than that of the central one, i.e., the $1a_1$ MO. Accordingly, the second peak at 536 eV may arise from the central O atom. However, the 536 eV band is convoluted at least by two Gaussian functions peaked at 535.4 and 536.3 eV.

Thus, electronic structure of the core-ionized and the core-excited states of O_3 were obtained by *ab initio* SCF calculations by using the code named GSCF3 [2, 3]. The calculations predict there exist six excited states below the K edge: two π^* and four σ^* states. Taking account of the IP difference between the central and the terminal O atoms, we assign the 535.4 eV band as the excitation to the π^* level from the center O(1*s*) MO. By comparing the term values obtained experimentally and theoretically in table 1, the proposed assignments are given in the last column.

Support of this work by New Energy and Industrial Technology Development Organization (NEDO) is gratefully acknowledged. We thank Prof. Kosugi, Dr. Adachi and Mr. Hatsui at IMS for technical assistance and for helpful discussions.

Reference

[1] M. S. Banna, D. C. Frost, C. A. McDowell, L. Noodleman and B. Wallbank, *Chem. Phys. Letters* 49 (1977) 213

[2] N. Kosugi and H. Kuroda, *Chem. Phys. Letters* 74 (1080) 490

[3] N. Kosugi, *Theor. Chim. Acta* 72 (1987) 149

Table 1. Peak positions, term values, effective principal quantum number n*, term values in the SCF calculation, and the proposed assignments.

Experiment			*ab initio* SCF calc.	Proposed assignments
Peak position (eV)	Term value (eV)	n*	Term value (eV)	
529.1	12.4(O_T)		12.0(O_T)	$\pi^*(2b_1) \leftarrow 2a_1$
535.4	10.8(O_C)		13.4(O_C)	$\pi^*(2b_1) \leftarrow 1a_1$
536.3	5.2(O_T)	1.6	3.9(O_T)	$\sigma^*(7a_1) \leftarrow (2a_1/1b_2)$
-	-	-	0.7(O_T)	$\sigma^*(5b_2) \leftarrow 2a_1$
541.5[a](O_T)				$(2a_1)^{-1}$ or $(1b_2)^{-1}$
542.31.9	3.9(O_C)	1.9	3.4(O_C)	$\sigma^*(7a_1) \leftarrow 1a_1$
544.02.5	2.2(O_C)	2.5	1.6(O_C)	$\sigma^*(5b_2) \leftarrow 1a_1$
546.2[a](O_C)				$(1a_1)^{-1}$

[a] Taken from ref. 1

(BL8B1) Vibration-resolved yield spectra of fragment ions from N_2 around the N1s to π^* resonance

Norio Saito[A] and Tatsuo Gejo

Institute for Molecular Science, Myodaiji, Okazaki 444-8585
[A] *Electrotechnical Laboratory, Umezono, Tsukuba-shi, 305-0045*

Resolution power of a soft X-ray monochromator has been developed and vibration-resolved spectra of several molecules have been obtained in these years. The fragment ion yield spectra from CO around the C-K edge shows dependence on vibration levels of excited states.[1] In this report, we have measured vibration-resolved fragment and parent ion yield spectra of N_2 around the N1s to π^* resonance.

The experiment has been performed at the beam line BL8B1 of UVSOR. A time-of-flight (TOF) mass spectrometer was used to obtain fragment ion yield spectra. An effusive flow of N_2 was introduced into the spectrometer at the presser of 2×10^{-5} Torr. A high field was applied in the collision region of the spectrometer so as to collect all kinetic ions. TOF of ions was measured with a TAC. The output pulse height from the TAC was analyzed with a MCA and SCA's. The windows of the SCA's were tuned so as to receive a pulse corresponding to N^{2+}, N^+, and N_2^+. The signals of the SCA's were counted and transferred to a computer.

Figure 1 shows an example of a TOF mass spectrum of N_2 measured at the excitation from 1s to $2p\pi_g(v=0)$. The dominantly produced ion is N^+. Yields of N^{2+} and N_2^+ are about 10% of that of N^+.

Figure 2 shows vibration-resolved ion yield spectra of N^{2+}, N^+, and N_2^+. The dots shows the experimental data and the solid curves are fitted with the Voigt function. The profiles of the N_2^+ spectrum are slightly different from those of the other spectra. These profiles agree with unpublished data measured by Saito *et al.*[2]

Reference

1) N.Saito, F.Heiser, O.Hemmers, A.Hempelmann, K.Wieliczek, J.Viefhaus, and U.Becker., Phys. Rev. A, **51**, R4313 (1995).
2) N.Saito, F.Heiser, and U.Becker, to be published.

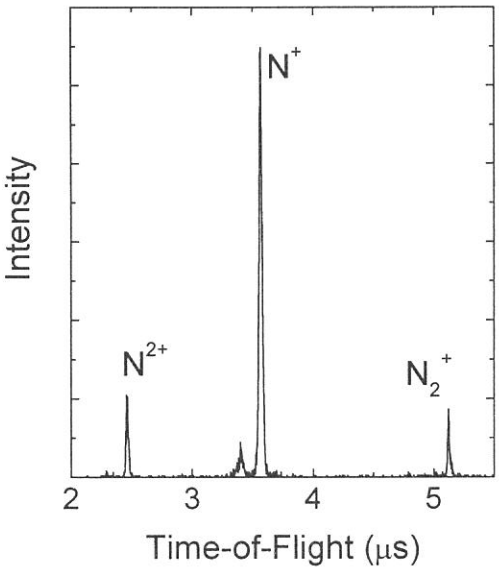

Fig.1 a TOF mass spectrum of N_2 measured at the excitation from 1s to $2p\pi_g(v=0)$.

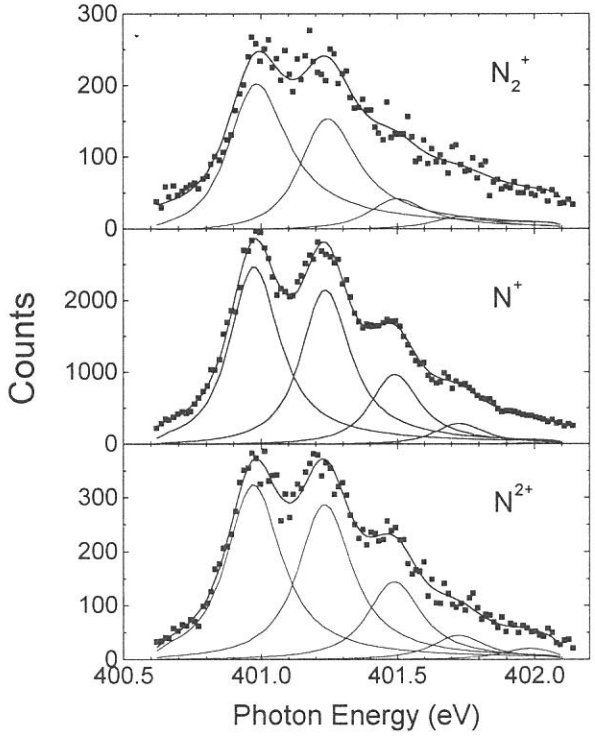

Fig.2 Vibration-resolved ion yield spectra of N^{2+}, N^+, and N_2^+ at the π^* resonance.